The Microstructure and Performance of Coal-Based Activated Carbon in Symmetric Supercapacitors as Affected by Activation Temperature and ZnCl2 Concentration

Markus Diantoro(✉), Rizka Ramadhani Maisyarah, and Ishmah Luthfiyah

Department of Physics, Faculty of Mathematics and Natural Sciences, Universitas Negeri Malang, Jl. Semarang 5, Malang, East Java 65145, Indonesia
markus.diantoro.fmipa@um.ac.id

Abstract. Supercapacitors are gaining much attention as electrochemical energy storage for their fast charging rates, high power density, good cycle performance, quicker charge-discharge, longer device life, and abundant materials. According to the storage mechanism, supercapacitors are divided into 3 types; EDLC (Electric Double Layer Capacitor), pseudocapacitor, and hybrid. Activated carbon is an excellent candidate as the primary material for making EDLC supercapacitors, and coal is one of the best precursor materials. Activated carbon can be synthesized by chemical and physical activation, where KOH and $ZnCl_2$ are often widely used. However, several researchers have studied the manufacture of activated carbon using $ZnCl_2$ activators still using a low temperature respectively, under 500°C. However, pore development is influenced by temperature. This research focuses on synthesizing activated carbon from coal using a ZnCl2 activator with different temperature variations at room temperature, 500, 800, and 1100°C. Briefly, the experiment begins with synthesizing coal-activated carbon with temperature variations. Then, the powder obtained was carried out by microstructure measurement, including SEM and XRD. The prime is the primary material for making electrodes and deposited on nickel foam to know its electrochemical performance. Furthermore, the electrodes are arranged with the separator and electrolyte into a coin cell device for electrochemical characteristics to be carried out. The electrochemical measurements include Cyclic Voltammetry (CV), Charge-Discharge (CD), and Electrochemical Impedance Spectroscopy (EIS) using the Gamry potentiostat and Battery Testing Equipment instruments.

Keywords: Coal · Activation Temperature · ZnCl2 Concentration · Symmetric Supercapacitor · Microstructure · Electrochemical Performance

1 Introduction

Harvesting energy from unlimited natural sources such as wind, solar, and geothermal requires storage devices that are flexible, portable, and environmentally friendly. This need encourages the attention of researchers and the government to develop research

A. Doyan et al. (Eds.): ICSES 2022, APR 8, pp. 157–165, 2023.
https://doi.org/10.2991/978-94-6463-232-3_16

related to storage technology that can be used for various energy sources [1, 2]. Supercapacitors are gaining much attention as electrochemical energy storage for their fast charging rates, high power density, good cycle performance, good durability charge, and natural abundance [3–5]. Supercapacitors with coin cell designs are broadly used as commercial designs for supercapacitors because they are suitable for supplying energy to small devices [6].

According to the storage mechanism, supercapacitors are divided into 3 types; EDLC (Electric Double Layer Capacitor), pseudocapacitor, and hybrid. Besides, activated carbon is the most suitable choice as the active material for EDLC supercapacitors, and coal is one of the best precursor materials. Activated carbon is a porous material containing 85–95% carbon with a large surface area consisting of free carbon elements covalently bonded. [7]. Activated carbon is obtained by activating precursor materials that contain high carbon concentrations and low inorganic compounds [7, 8]. The precursor material that is widely used comes from biomass waste. Previous studies reported the use of biomass waste as a material for making activated carbon, including rice husks [9–11], wood sawdust [13], coconut shells [16], durian shells [17–19], and many more. However, activated carbon from coal has superior performance compared to biomass-activated carbon because it has a larger pore size [12, 13]. As one of the world's leading coal-producing nations, Indonesia has abundant coal reserves of up to around 26 billion tons [14]. These potential coal reserves are mostly found on the island of Kalimantan, where there are reserves of up to 62.1% of the total potential of Indonesia's coal reserves.

Activated carbon is synthesized through two processes, namely carbonization, and activation. Carbonization is accomplished between 300 and 800°C, producing flexible charcoal with a low surface area and adsorption ability [15]. Therefore, different activation processes, both physical and chemical, are needed. Chemical activation is carried out by adding acids, bases, or salts such as HCl, H3PO4, KOH, K2CO3, ZnCl2, and others [16]. ZnCl2 activator functions as Lewis acid which increases the aromatic condensation reaction and inhibits the formation of volatile compounds so that the activated carbon obtained is greater than using KOH.

From the research that has been reported, the manufacture of activated carbon using ZnCl2 activator still uses a fairly long and complicated method, which involves nitric acid, pyrolysis, inert gas, or large concentrations of ZnCl2 [17–20]. However, several researchers have studied the manufacture of activated carbon using ZnCl2 activators still using a low temperature respectively, under 500°C. Although the pore development is influenced by temperature. Therefore it is necessary to research the manufacture of activated carbon using a ZnCl2 activator more simply and study the effect of activation temperature on its performance. In this study, coal was utilized as a precursor material, and the activation temperature was varied to investigate the relationship between the activation temperature and the microstructure. Then the prime one was fabricated as a supercapacitor to know its electrochemical performance.

2 Method

2.1 Activated Coal Carbon Preparation

Bituminous coal stones were ground to a fine powder and sieved to 200 mesh. Then coal powder was carbonized in a chamber furnace for 90 min at 650°C without inert gas flowed and subsequently impregnated for 1 day in $ZnCl_2$ with a ratio of 0.01:2. Afterwards, it activated at various temperatures (500, 800, 1100°C). It washed properly until we got normal pH. For the next step, we call the samples T500, T800, and T1100 for activated temperatures 500, 800, dan 1100°C. The microstructure measurement was carried out using XRD with Cu anode, 1-degree slit divergence, receiving slit 0.2 mm X'Pert PRO (Pan Analytical), and SEM FEI type INSPECT-S50.

The T1100 powder was then used as the primary material to make the electrode using the blending method with a ratio of 8:1:1 for the active material in the form of activated coal carbon, conductive material, and binder using N-Methyl-2-pyrrolidone (NMP) as solvent at R.T., then mixed for 20 h straight. Then, the black slurry was cast on nickel foam as a substrate using a micro pipet on both sides and dried at 80°C for 1 h in an oven. Afterward, the prepared electrodes were punched into circular discs, and electrochemical measurements of symmetric coal supercapacitors were carried out using a coin-type cell (2032) with KOH as an electrolyte. The electrochemical measurement was carried out using Gamry Instrument and Neware Battery Testing. The electrochemical test of these electrodes was investigated by cyclic voltammetry (CV) measurements on the T1100 sample with a voltage range of 0–1.0 V at various scan rates 10, 20, and 30 mV s^{-1} and Charge-Discharge performance was carried out on 1,5 maximum voltage. (The test was conducted at room temperature).

3 Results and Discussion

Figure 1 shows the diffraction pattern of activated coal activated carbon using $ZnCl_2$ with temperature variations of 0 (without temperature), 500, 800, and 1100°C. The diffraction pattern of activated carbon has a semicrystalline phase, whereas the semicrystalline phase

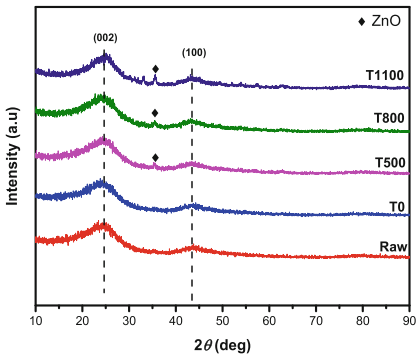

Fig. 1. Diffraction Pattern of Coal Activated Carbon Powder with Temperature Activation Variated

shows a phase between amorphous and crystalline. A peak indicates the crystalline phase at a certain angle of 2θ, but the peak is wide and sloping, indicating the presence of an amorphous phase. The results of the study obtained 2 peaks in the plane (002) and (100) with an angle of 2θ in the range of 24.33–25.09° and 43.49–43.55, which confirmed by previous studies [21–24]. The fields (002) and (100) indicate the formation of a turbostatic structure [25]. In addition, in the low 2θ scattering angle, the intensity is greater, which indicates the presence of many pores in the mesoporous category [26, 27].

There is a peak of ZnO at angles of 32.95° and 35.63°, indicating that Zn is present on the sample surface. ZnO, however, only hit its peak in samples with varying activation temperatures, where the peak's strength rose as activation temperature rose. This is consistent with $ZnCl_2$'s characteristic, which states that beyond 400°C, $ZnCl_2$ will evaporate and partly oxidize to ZnO [28]. The existence of a ZnO peak, where the crystallinity of ZnO rises with increasing activation temperature, from 3% to 17%, is also confirmed by Fig. 2. According to other investigations [21, 29], the occurrence of ZnO peaks during activated carbon activation using the $ZnCl_2$ activator is aligned.

The surface morphology of powdered coal-activated carbon using ZnCl2 with variations in room temperature, 500, 800, and 1100°C, is shown in Fig. 3 (a–d).

The mesoporous pores on the surface of the activated carbon T0 coal particles, which have a stone-like morphology as seen in Fig. 3 (a), are numerous and uniformly sized at 4.63 m. The surface morphology of activated carbon made from powdered coal is shown in Fig. 4 3 (b–e) at activation temperatures of 500, 800, and 1100°C. The pore diameters of samples T0, T500, T800, and T1100 are 2.52, 7.37, 7.37, and 8.03 μm, respectively. Figure 3 (b–e) illustrates the impact of temperature treatment on coal-activated carbon. The four samples were classified as macropores. The surface of Sample T1100 is formed like a cork, which improves the adsorption of activated carbon and has the biggest pore diameter. The larger the pore, the larger the active surface, then ion transfer will occur faster [30, 31].

Figure 4 (a) shows a leaf-like shape or semi-rectangular (quasi-rectangular), which indicates that the activated carbon electrode is included in the EDLC type supercapacitor

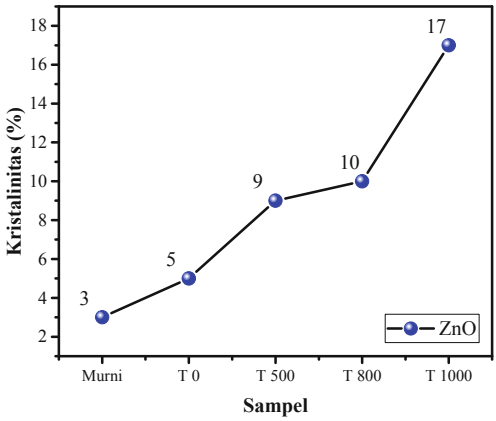

Fig. 2. Graph of Crystallinity to Activation Temperature

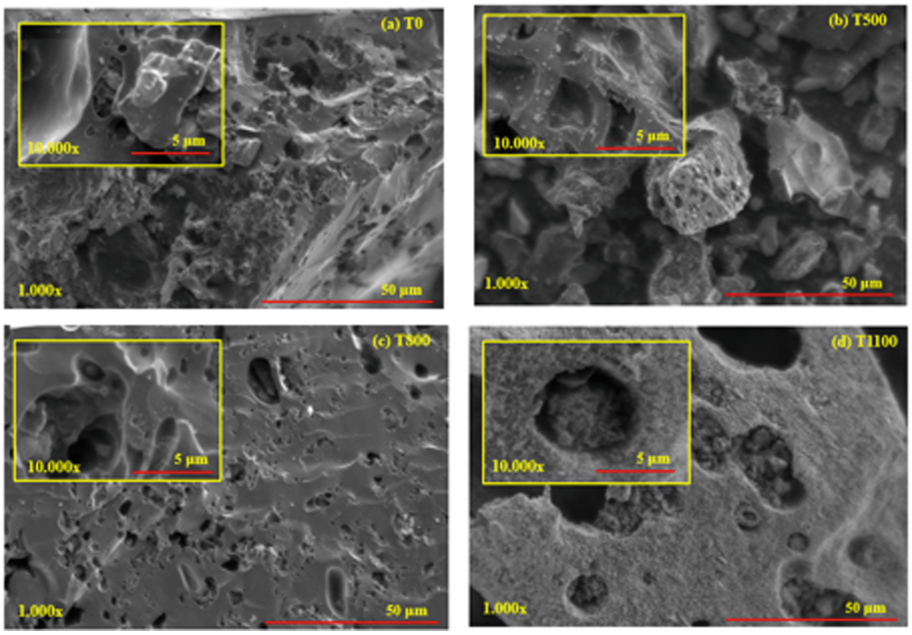

Fig. 3. The morphology of coal-activated carbon with variations of (a) T0, (b) T500, (c) T800, and (d) T1100.

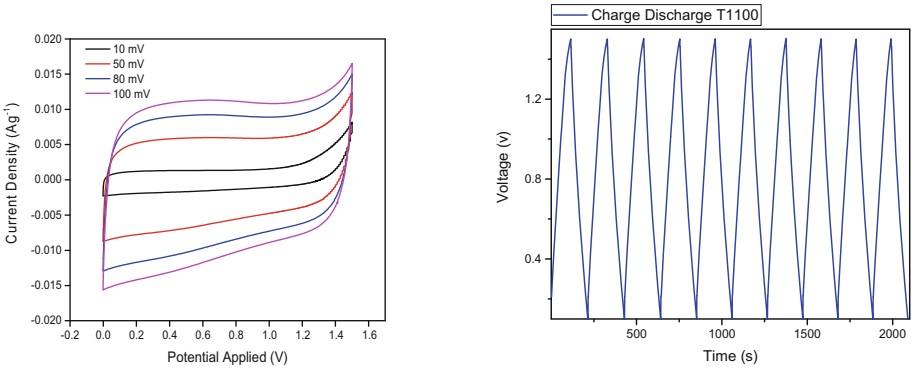

Fig. 4. (a) CV Curve with scan rate variation (b) CD Curve for sample T1100

and shows the properties of the EDLC pseudocapacitance device which has good capacitive capability [32, 33]. This capacitive ability is influenced by the accumulation of charge in storage, which occurs by forming two interfacial layers between the electrode and the electrolyte without a faradaic peak so that no redox reactions occur [34]. Also, Fig. 4 (a) displays the CV curve of T1100 at different scan rate applications, namely 10, 50, 80, and 100 mVs−1. The curve at a scan rate of 10–100 mVs−1 is well-formed without any disconnection, indicating an increase in electron conduction that supports

the speed of charge diffusion on the electrode so that the capacitive performance of the electrode is stable [35, 36]. This transfer rate also affects the capacitance value, where the capacitance value drops with increasing scan rate. At low scan rates, the charging and discharging speed is slower so that the K+ and O.H− ions in the electrolyte have enough time to diffuse to obtain a higher specific capacitance value. While at a higher scan rate, the charging and discharging process takes place quickly, which results in less utilization of the electrode surface, so a lower specific capacitance value is obtained [37–39].

Figure 4b shows the results of the charge-discharge test on coal-activated carbon with variations in activation temperature 1100 °C at a current density of 1 Ag−1 and 1 M KOH as the electrolyte solution. The charge-discharge curve is formed based on the voltage (V) and time (s) relationship. In the picture, the CD curve is shaped almost like an equilateral triangle which indicates the characteristics of the EDLC supercapacitor electrode [40, 41]. Ideally, the charge time should equal the discharge time. However, in Fig. 4b, the charging time is longer, and there are bumps in a certain voltage range, which is unequal to the discharge time. This is due to the pseudocapacitive effect of the oxygen heteroatoms present in the sample [42]. Also, it has good stability, as shown by the curve, which has a regular size. The CV and CD tests found that the specific capacitance, energy density, and power density values reached 28.205 Fg-1, respectively; 7,145 Whkg−1; 275,310 Wkg−1 for T1100. A sudden voltage drop, commonly called an I.R. drop, occurs in the phase of charge transfer to discharge due to a combination of electrode resistance, electrolyte, ion transfer in the electrode material, and contact voltage in the electrochemical system [43]. The T1100 activated carbon electrode has the smallest I.R. drop value of 0.0428 V, which indicates that ion transfer occurs quickly, so it has good electrochemical performance and electrical conductivity.

4 Conclusion

In summary, we have developed that adding the activation temperature in the coal activation process can improve the microstructure and electrochemical performance of the activated carbon produced. Pore size increases with increasing activation temperature. Where a pore is formed in the macropore category, with the largest diameter being 8,03 μm, with a cork-like shape on sample T1100. Electrochemical measurement results indicate activated coal carbon with 1100°C temperature activation shows a good result with specific capacitance, energy density, and power density values reaching 28.205 Fg^{-1}, respectively; 7,145 $Whkg^{-1}$; 275,310 Wkg^{-1}.

Acknowledgments. The authors should thank the government of the Republic of Indonesia through the Research Grant of PNBP of the Universitas Negeri Malang.

References

1. G. Z. Chen, "Supercapacitor and supercapattery as emerging electrochemical energy stores," Int. Mater. Rev., vol. 62, no. 4, pp. 173–202, May 2017, https://doi.org/10.1080/09506608.2016.1240914.
2. L. Yu and G. Z. Chen, "Supercapatteries as High-Performance Electrochemical Energy Storage Devices," Electrochem. Energy Rev., vol. 3, no. 2, pp. 271–285, Jun. 2020, https://doi.org/10.1007/s41918-020-00063-6.
3. Y. Kado, Y. Soneda, H. Hatori, and M. Kodama, "Advanced carbon electrode for electrochemical capacitors," J. Solid State Electrochem. 2019 234, vol. 23, no. 4, pp. 1061–1081, Feb. 2019, https://doi.org/10.1007/S10008-019-04211-X.
4. D. Wu et al., "MnO2/Carbon Composites for Supercapacitor: Synthesis and Electrochemical Performance," Front. Mater., vol. 7, no. February, pp. 1–16, 2020, https://doi.org/10.3389/fmats.2020.00002.
5. Suhdi and S. C. Wang, "Fine activated carbon from rubber fruit shell prepared by using zncl2 and koh activation," Appl. Sci., vol. 11, no. 9, 2021, https://doi.org/10.3390/app11093994.
6. V. Murray, D. S. Hall, and J. R. Dahn, "A Guide to Full Coin Cell Making for Academic Researchers," J. Electrochem. Soc., vol. 166, no. 2, pp. A329–A333, 2019, https://doi.org/10.1149/2.1171902jes.
7. W. Bae, J. Kim, and J. Chung, "Production of granular activated carbon from food-processing wastes (walnut shells and jujube seeds) and its adsorptive properties," J. Air Waste Manag. Assoc., vol. 64, no. 8, pp. 879–886, 2014, https://doi.org/10.1080/10962247.2014.897272.
8. O. Ioannidou and A. Zabaniotou, "Agricultural residues as precursors for activated carbon production-A review," Renew. Sustain. Energy Rev., vol. 11, no. 9, pp. 1966–2005, 2007, https://doi.org/10.1016/j.rser.2006.03.013.
9. J. Alvarez, G. Lopez, M. Amutio, J. Bilbao, and M. Olazar, "Upgrading the rice husk char obtained by flash pyrolysis for the production of amorphous silica and high quality activated carbon," Bioresour. Technol., vol. 170, pp. 132–137, 2014, https://doi.org/10.1016/J.BIORTECH.2014.07.073.
10. M. M. Rahman, Q. HamidulBari, N. Mohammad, A. Ahsan, H. R. Sobuz, and M. Alhaz Uddin, "Characterization of Rice Husk Carbon Produced through Simple Technology," Adv. Mater. Sci. Appl., vol. 2, no. 1, pp. 25–30, Mar. 2013, https://doi.org/10.5963/AMSA0201003.
11. M. . Tadda et al., "A Review on Activated Carbon from Biowaste : Process , Application and Prospects," J. Adv. Civ. Eng. Pract. Res., vol. 5, no. 3, pp. 82–83, 2018.
12. K. Amstaetter, E. Eek, and G. Cornelissen, "Sorption of PAHs and PCBs to activated carbon: Coal versus biomass-based quality," Chemosphere, vol. 87, no. 5, pp. 573–578, 2012, https://doi.org/10.1016/J.CHEMOSPHERE.2012.01.007.
13. H. Teng, J. A. Ho, Y. F. Hsu, and C. T. Hsieh, "Preparation of Activated Carbons from Bituminous Coals with CO2 Activation. 1. Effects of Oxygen Content in Raw Coals," Ind. Eng. Chem. Res., vol. 35, no. 11, pp. 4043–4049, 1996, https://doi.org/10.1021/IE960170D.
14. ESDM, "Kementerian ESDM RI - Media Center - Arsip Berita - Cadangan Batubara Indonesia Sebesar 26 Miliar Ton," 2018. https://www.esdm.go.id/id/media-center/news-archives/cadangan-batubara-indonesia-sebesar-26-miliar-ton (accessed Jun. 23, 2022).
15. H. T. Ma et al., "Effect of the Carbonization and Activation Process on the Adsorption Capacity of Rice Husk Activated Carbon," Vietnam J. Sci. Technol., vol. 55, no. 4, 2017, https://doi.org/10.15625/2525-2518/55/4/9124.
16. S. Sunarsih et al., "Activated Carbon from Jackfruit Peel Waste ss Decolouring Agent of Screen Printing Waste Water," Semin. Nas. Tek. Kim. Kejuangan, vol. 0, no. 0, p. 7, 2016, [Online]. Available: http://jurnal.upnyk.ac.id/index.php/kejuangan/article/view/1560.

17. S. Sundari Gunasekaran, R. Subashchandra Bose, and K. Raman, "Electrochemical Capacitive Performance of ZnCl2 Activated Carbon Derived from Bamboo Bagasse in Aqueous and Organic Electrolyte," Orient. J. Chem., vol. 35, no. 1, pp. 302–307, 2019, https://doi.org/10.13005/ojc/350136.
18. I. I. G. Inal, S. M. Holmes, A. Bamford, and Z. Aktas, "The performance of supercapacitor electrodes developed from chemically activated carbon produced from waste tea," Appl. Surf. Sci., vol. 357, pp. 696–703, 2015.
19. E. Taer et al., "The synthesis of activated carbon made from banana stem fibers as the supercapacitor electrodes," Mater. Today Proc., vol. 44, pp. 3346–3349, 2020, https://doi.org/10.1016/J.MATPR.2020.11.645.
20. T. E. Rufford, D. Hulicova-Jurcakova, K. Khosla, Z. Zhu, and G. Q. Lu, "Microstructure and electrochemical double-layer capacitance of carbon electrodes prepared by zinc chloride activation of sugar cane bagasse," J. Power Sources, vol. 195, no. 3, pp. 912–918, 2010, https://doi.org/10.1016/j.jpowsour.2009.08.048.
21. R. Rajbhandari, L. K. Shrestha, and R. R. Pradhananga, "Nanoporous activated carbon derived from lapsi (choerospondias axillaris) seed stone for the removal of arsenic from water," J. Nanosci. Nanotechnol., vol. 12, no. 9, pp. 7002–7009, 2012, https://doi.org/10.1166/jnn.2012.6568.
22. A. I. Bakti, P. L. Gareso, and N. Rauf, "Characterization of Active Carbon from Coconut Shell using X-Ray Diffraction (X-RD) and SEM-EDX Techniques," J. Penelit. Fis. dan Apl., vol. 8, no. 2, p. 115, Dec. 6368, https://doi.org/10.26740/JPFA.V8N2.P115-122.
23. G. Krishna Gupta et al., "In Situ Fabrication of Activated Carbon from a Bio-Waste Desmostachya bipinnata for the Improved Supercapacitor Performance," Nanoscale Res Lett, vol. 16, p. 85, 2021, https://doi.org/10.1186/s11671-021-03545-8.
24. H. Shang, Y. Lu, F. Zhao, C. Chao, B. Zhang, and H. Zhang, "Preparing high surface area porous carbon from biomass by carbonization in a molten salt medium," RSC Adv., vol. 5, no. 92, pp. 75728–75734, Sep. 2015, https://doi.org/10.1039/C5RA12406A.
25. R. Wang et al., "A cost effective, highly porous, manganese oxide/carbon supercapacitor material with high rate capability," J. Mater. Chem. A, vol. 4, no. 15, pp. 5390–5394, 2016.
26. Y. Zhai, Y. Dou, D. Zhao, P. F. Fulvio, R. T. Mayes, and S. Dai, "Carbon Materials for Chemical Capacitive Energy Storage," Adv. Mater., vol. 23, no. 42, pp. 4828–4850, Nov. 2011, https://doi.org/10.1002/ADMA.201100984.
27. S. Schimmelpfennig and B. Glaser, "One Step Forward toward Characterization: Some Important Material Properties to Distinguish Biochars," J. Environ. Qual., vol. 41, no. 4, pp. 1001–1013, 2012, https://doi.org/10.2134/jeq2011.0146.
28. F. Jones, H. Tran, D. Lindberg, L. Zhao, and M. Hupa, "Thermal stability of zinc compounds," Energy and Fuels, vol. 27, no. 10, pp. 5663–5669, 2013, https://doi.org/10.1021/ef400505u.
29. A. I. Bakti and P. L. Gareso, "Characterization of Active Carbon Prepared from Coconuts Shells using FTIR, XRD and SEM Techniques," J. Ilm. Pendidik. Fis. Al-Biruni, vol. 7, no. 1, pp. 33–39, Apr. 2018, https://doi.org/10.24042/JIPFALBIRUNI.V7I1.2459.
30. S. Majid, A. S. G. Ali, W. Q. Cao, R. Reza, and Q. Ge, "Biomass-derived porous carbons as supercapacitor electrodes-A review," Xinxing Tan Cailiao/New Carbon Mater., vol. 36, no. 3, pp. 546–572, Jun. 2021, https://doi.org/10.1016/S1872-5805(21)60038-0.
31. Y. Tan et al., "Reaction kinetics in rechargeable zinc-ion batteries," J. Power Sources, vol. 492, Apr. 2021, https://doi.org/10.1016/J.JPOWSOUR.2021.229655.
32. M. Ashraf et al., "A High-Performance Asymmetric Supercapacitor Based on Tungsten Oxide Nanoplates and Highly Reduced Graphene Oxide Electrodes," Chem. - A Eur. J., vol. 27, no. 23, pp. 6973–6984, Apr. 2021, https://doi.org/10.1002/CHEM.202005156.
33. X. Liang et al., "BaTiO3 internally decorated hollow porous carbon hybrids as fillers enhancing dielectric and energy storage performance of sandwich-structured polymer composite," Nano Energy, vol. 68, Feb. 2020, https://doi.org/10.1016/J.NANOEN.2019.104351.

34. J. Sung and C. Shin, "Recent studies on supercapacitors with next-generation structures," Micromachines, vol. 11, no. 12, pp. 1–25, Dec. 2020, https://doi.org/10.3390/MI11121125.
35. M. Chen, Q. Cheng, Y. Qian, J. He, and X. Dong, "Alkali cation incorporated MnO2 cathode and carbon cloth anode for flexible aqueous supercapacitor with high wide-voltage and power density," Electrochim. Acta, vol. 342, p. 136046, May 2020, https://doi.org/10.1016/J.ELECTACTA.2020.136046.
36. L. Sun et al., "From coconut shell to porous graphene-like nanosheets for high-power supercapacitors," J. Mater. Chem. A, vol. 1, no. 21, pp. 6462–6470, Jun. 2013, https://doi.org/10.1039/c3ta10897j.
37. B. Yang et al., "Ecotoxicology and Environmental Safety Evaluation of activated carbon synthesized by one-stage and two-stage co-pyrolysis from sludge and coconut shell," Ecotoxicol. Environ. Saf., vol. 170, no. August 2018, pp. 722–731, 2019, https://doi.org/10.1016/j.ecoenv.2018.11.130.
38. Y. Xie and H. Du, "Electrochemical capacitance of a carbon quantum dots-polypyrrole/titania nanotube hybrid," RSC Adv., vol. 5, no. 109, pp. 89689–89697, 2015, https://doi.org/10.1039/C5RA16538E.
39. J. J. Huang, Y. X. Zhang, and J. X. Zhang, "Characterization of MnO2 and AgNWs Co-Doped into an Activated Carbon Thin Film Electrode for Supercapacitors," J. Electron. Mater. 2021 5011, vol. 50, no. 11, pp. 6535–6544, Sep. 2021, https://doi.org/10.1007/S11664-021-09202-1.
40. J. Jose, V. Thomas, V. Vinod, R. Abraham, and S. Abraham, "Nanocellulose based functional materials for supercapacitor applications," J. Sci. Adv. Mater. Devices, vol. 4, no. 3, pp. 333–340, Sep. 2019, https://doi.org/10.1016/J.JSAMD.2019.06.003.
41. Z. Gao, Y. Zhang, N. Song, and X. Li, "Biomass-derived renewable carbon materials for electrochemical energy storage," http://mc.manuscriptcentral.com/tmrl, vol. 5, no. 2, pp. 69–88, Mar. 2016, https://doi.org/10.1080/21663831.2016.1250834.
42. L. Wan et al., "Facile synthesis of nitrogen self-doped hierarchical porous carbon derived from pine pollen via MgCO3 activation for high-performance supercapacitors," J. Power Sources, vol. 438, Oct. 2019, https://doi.org/10.1016/J.JPOWSOUR.2019.227013.
43. K. Yang, K. Cho, D. S. Yoon, and S. Kim, "Bendable solid-state supercapacitors with Au nanoparticle-embedded graphene hydrogel films," Sci. Rep., vol. 7, Jan. 2017, https://doi.org/10.1038/SREP40163